Asian Journal of Chemistry; Vol. 36, No. 7 (2024), 1483-1488

ASIAN JOURNAL OF CHEMISTRY

https://doi.org/10.14233/ajchem.2024.31450

Garcinia indica Leaf Extract Derived Ag-Zn Nanocomposites: A Sustainable Approach for Textile Dyes Photodegradation

J.T. KURIAN and K.S. JOSEPH*

Department of Life Sciences, Christ University, Bangalore-560029, India

*Corresponding author: E-mail: joseph.ks@christuniversity.in

Received: 27 February 2024; *Accepted*: 8 April 2024; *Published online*: 29 June 2024; AJC-21664

The recent advancements for the biosynthesis of nanoparticles from plant biomass offer a promising avenue for the sustainable and environmentally friendly production of nanomaterials. The utilization of plant extracts as bioreductants and capping agents leverages naturally occurring biomolecules for the controlled synthesis of nanoparticles, minimizing environmental impacts and promoting a more sustainable nanotechnology landscape. This study explores the biofabrication of silver-zinc nanocomposites (Ag-Zn NCs) using *Garcinia indica* leaf extract, offering a green and sustainable alternative to conventional methods. The synthesized nanocomposites were characterized using UV-vis, FTIR, XRD and TEM analyses. The UV-vis spectra confirmed the formation of nanocomposites with distinct surface plasmon resonance peaks (355 nm and 408 nm). FTIR identified functional groups involved in the bioreduction, while XRD indicated a crystalline size of 6.26 nm. TEM images revealed a mixture of hexagonal, spherical and rod-shaped nanocomposites with an average size of 40.37 nm. Furthermore, the study evaluated the photocatalytic activity of the Ag-Zn NCs against various reactive textile dyes (RY-86, RY-145, RB-220 and RB-222). Remarkably, the nanoparticles achieved an impressive 87-100% degradation of these dyes within 160-320 min under UV irradiation. This highlights the potential of biofabricated Ag-Zn NCs for environmental remediation, particularly in treating dye contaminated industrial effluents. This work demonstrates the feasibility of using *G. indica* leaf extract for the sustainable synthesis of Ag-Zn NCs with efficient dye degradation capabilities.

Keywords: Nanocomposites, Green synthesis, *Garcinia indica,* Photocatalytic, Reactive textile dyes, Chemical kinetics.

INTRODUCTION

The growing field of nanotechnology offers exciting solutions for environmental remediation and the application of metal and metal oxide nanocomposites (MNMs) as photocatalysts holds immense potential in this arena [1,2]. Water pollution, particularly from industrial effluents, poses a significant threat to human well-being and ecosystem health [3]. The ability to fine-tune properties by combining different MNMs allows for targeted applications, such as photocatalysis, enhanced antimicrobial activity and exploration of novel functionalities [4-7]. MNMs offer promising solutions for colorimetric sensing of heavy metals and degradation of organic dyes, addressing major water pollution concerns [8].

Reactive azo dyes, widely used for colouring textiles, pose a specific challenge due to their high molecular weight and resistance to biodegradation. This persistence allows them to accumulate in water bodies, leading to potential adverse effects on aquatic ecosystems and human health [9]. Traditional effluent treatment methods, while providing some level of pollutant removal, are often insufficient in addressing the diverse and complex pollutants present in industrial wastewater [5,10]. Therefore, the development and implementation of novel, more efficient and sustainable technologies for effluent treatment is crucial to mitigate the environmental and health impacts of industrial activities.

Ag-ZnO nanocomposites are attracting attention due to the synergistic combination of their individual functionalities. ZnO serves as a cost-effective 3D support, offering high charge carrier mobility, longer electron lifetimes and mild catalytic behaviour [5,11]. The use of silver nanoparticles enhances performance by serving as electron decreases, enhancing photocatalytic activity and prolonging the retention duration of electron-hole pairs. This synergistic approach opens avenues for developing highly efficient nanomaterials with applications in diverse fields like environmental remediation, energy conv-

ersion and antibacterial treatments [8]. Green synthesis techniques provide a number of benefits, including the utilization of readily available and reasonably priced plant extracts, a large diversity of naturally occurring phytochemicals and the lack of hazardous reagents [10].

Garcinia indica, commonly known as kokum, is a fruit-bearing tree belonging to the Clusiaceae family. It holds significance in culinary, pharmaceutical and industrial domains and is primarily found in the Western Ghats of India. The plant is renowned for its richness in phytocompounds with hydroxycitric acid and garcinol being the most studied for their antimicrobial and cytotoxic properties [12]. The presence of flavonoids, xanthones, benzophenones, bioflavonoids and triterpenoids in *G. indica* extracts has been documented by FTIR studies [13]. This study investigates the utilization of phytochemicals extracted from *G. indica* leaves for the biofabrication of silver-zinc oxide nanocomposites (Ag-Zn NCs).

Despite its widespread culinary use and easy accessibility, the present research focuses on *G. indica* leaf extracts. This choice stems from the authors' interest in exploring the unexplored potential of these leaves in the fields of sustainable nanotechnology and bioremediation aspects. By investigating the use of *G. indica* leaf extracts for biofabrication, this study opens avenues for exploring the unexploited potential of natural resources in nanotechnology and bioremediation.

EXPERIMENTAL

The leaves of *G. indica* were collected from the south canara of Karnataka state, India during summer. All the chemicals were procured from Sigma-Aldrich, India. Distilled water was used to prepare all the aqueous solutions. Prior to usage, all the glasswares were thoroughly cleaned, rinsed with distilled water and dried. All the studied dyes in this study *viz.* reactive yellow 86 (RY-86), yellow 145 (RY-145), reactive blue 220 (RB-220) and reactive blue 222 (RB-222) were procured from Merck, India.

Preparation of aqueous leaf extract: Particulate matter and organic contaminants were removed from the freshly harvested leaves by carefully washed them with distilled water. Subsequently, the rinsed leaves were subjected to shade drying, followed by oven drying at 35 ºC. The desiccated leaves were finely pulverized using a domestic grinder and stored in hermetically sealed containers. A 10 g of *G. indica* leaf powder was mixed with 300 mL of distilled water and the resulting mixture underwent reflux extraction at 50 ºC for 30 min. The resultant extract was filtered *via* Whatman No. 1 filter paper to obtain a filtered *G. indica* extract solution, which was used in the biosynthesis of Ag-Zn NCs [14].

Green synthesis of Ag-Zn NCs: A reaction mixture consisting of 100 mL of 0.5 M zinc acetate dihydrate and 100 mL of 0.05 M $AgNO_3$ was employed. Subsequently, 10 mL of *G. indica* leaf extract was incrementally introduced into the reaction mixture under magnetic stirring conditions. Sodium hydroxide was used as the pH stabilizing agent and the reaction mixture's pH was carefully regulated to a range of 10-11. The procedure was repeated multiple times until the initially greenish-black precipitate in the colloidal solution was obtained.The reaction was carried out with continuous stirring for an additional hour [15]. After removing the supernatant, the mixture was centrifuged for 10 min at 10,000 rpm to collect the pellets. This process was then repeated 5-6 times using ethanol and water to remove any remaining contaminants. After being washed, the pellets were again suspended in distilled water and dried at 60 ºC in a hot air oven [16]. The dried nanocomposites were further used for the photodegradation of textile dyes.

Characterization: A UV-vis absorption spectroscopic analysis (Shimadzu UV-1800ENG240V UV spectrophotometer) at 200-800 nm was used for the initial study of the biosynthesis of Ag-Zn NCs. A Shimadzu IR spectrophotometer operating at a scanning series of 4000-500 cm^{-1} was used to identify the biomolecules of *G. indica* extract and the produced Ag-Zn NCs. XRD analysis was performed using a Rigaku-Miniflex X-ray diffractometer in order to analyze the crystal phase data of the nanocomposites and the Debye-Scherrer equation was used to determine the crystal size of nanocomposite. The JEOL-JEM 2100 plus Transmission electron microscope was used to conduct TEM-SAED in order to gain a deeper comprehension of the surface morphology and crystalline properties of the synthesized nanocomposites.

Photocatalytic degradation of textile dyes: The photocatalytic effectiveness of synthesized Ag-Zn NCs was tested using water-based solutions containing reactive textile colouring compounds, including RY-86, RY-145, RB-220 and RB-222. A 10 mg of Ag-Zn NCs (1 mg/mL) were added to 10 mL solutions of the corresponding dyes at a 5 ppm concentration; dye solutions without the synthesized Ag-Zn NCs addition were used as control group. The nanocomposites and dye solutions underwent mixing using a magnetic stirrer in the absence of light for a duration of 10-15 min, followed by exposure to UV irradiation for 320 min with continuous stirring. The absorbance of each dye was quantified at designated time intervals (5, 10, 20, 40, 80, 160 and 320 min) using a UV-Vis spectrophotometer to monitor the progression of the photocatalytic reaction. The rate of degradation of reactive dyes by Ag-Zn NCs was determined by using the following formula [16]:

$$\text{Degradation } (\%) = \frac{A_o - A_t}{A_o} \times 100$$

where the absorbances of the test and control are denoted by A_t and A_o, respectively.

The pseudo-first-order kinetic was used to determine the kinetics and the rate of degradation of the textile dyes and can be represented as follows:

$$\ln\left(\frac{A_t}{A_o}\right) = -kt$$

where t is the time in minutes, k is the rate constant and A_t and A_0 represent the intial and final concentrations of dye over time.

RESULTS AND DISCUSSION

The aqueous extract derived from *G. indica* leaf is particularly rich in phytochemicals that serve as natural agents for reducing, capping and stabilizing metal nanoparticles and nanocomposites, offering an alternative to expensive chemical

additives in the synthesis process [5]. Upon addition of *G. indica* extract to the metal ion solution, the solution's colour shifted from light green to a greenish black hue, suggesting metal ion reduction. After adding NaOH till the pH reached 10, the colloidal solution turned entirely greenish black indicating the successful formation of Ag-Zn NCs [15].

UV-vis spectral studies: Fig. 1 depicts the absorption spectrum of the synthesized Ag-Zn NCs, providing the insights into their composition relying on their optical properties. The presence of a broad band around 408 nm is consistent with the characteristic surface plasmon resonance of silver nanoparticles, while the SPR peak at 355 nm matched with the expected absorption peak of ZnO nanoparticles, as reported in the literature [15,17]. At the same time the band observed at 276 nm might be due to unreacted metal ions or phytochemicals persisting in the reaction mixture. The proposed mechanism for the bioreduction of metal ions to nanocomposites suggests that the involvement of multiple polyphenolic compounds present in the biological extract facilitates the reduction process [17].

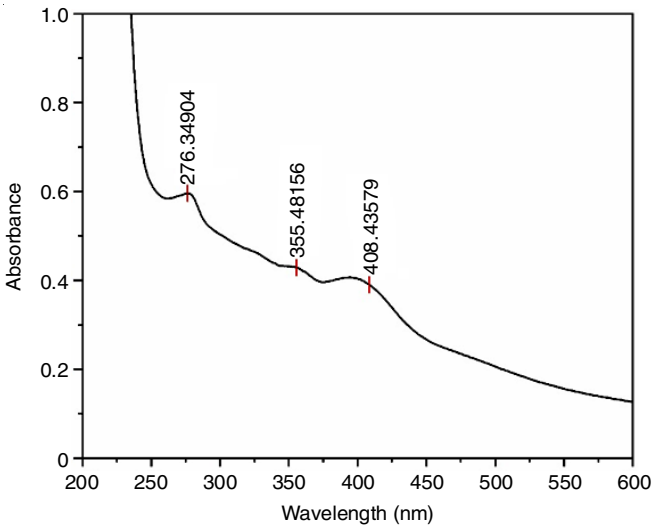

Fig. 1. UV-vis spectrum of the synthesized Ag-Zn nanocomposite from *Garcinia indica* leaf extract

FTIR spectroscopy: Fourier-transform infrared (FTIR) spectroscopy was employed to elucidate the biomolecules involved in the green synthesis of Ag-Zn NCs by analyzing the leaf extract of *G. indica* and the synthesized nanocomposite themselves (Fig. 2). The FTIR spectrum of the leaf extract revealed a broad, strong band at 3337.34 cm^{-1}, characteristic of O-H stretching in carboxylic acids. Additionally, distinct peaks at 2923.15 and 2852.45 cm^{-1} indicated C-H stretching of alkanes, while bands at 1740.52 and 1616.80 cm^{-1} confirmed the presence of C=O stretching in carboxylic acids. Further characteristic peaks were observed at 1436.21, 1244.10 and 1025.10 cm^{-1}, corresponding to O-H bending of carboxylic acids, C-N stretching of amines and CO-O-CO stretching of anhydrides, respectively. These findings collectively substantiate the presence of various phytochemicals in the garcinia extract, including flavonoids, xanthones, anthocyanins, benzophenones, biflavonoids, terpenoids, hydroxycitric acid and garcinol [13]. The FTIR spectrum of the green-synthesized Ag-Zn NCs closely

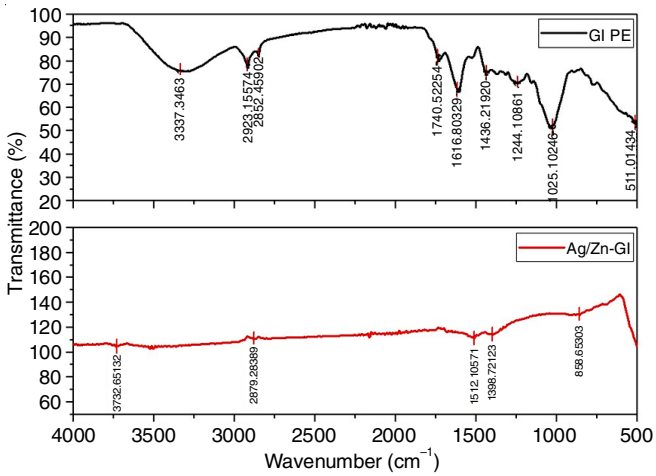

Fig. 2. FTIR spectra of the *Garcinia indica* leaf extract and the synthesized Ag-Zn nanocomposites

resembles that of the *G. indica* leaf extract. However, subtle shifts in peak positions towards lower wavenumbers and broadening of several bands are observed in the nanocomposites spectrum. Significantly, the nanocomposites exhibit additional bands at 3735.63 and 3510.65 cm^{-1}, indicative of O-H stretching vibrations in alcohols and N-H stretching vibrations in primary amines, respectively. Furthermore, a broadened band at 2975.36 cm^{-1}, assigned to C-H stretching in alkanes, is also present in the nanocomposites spectrum, mirroring the leaf extract. Additional characteristic peaks in the nanocomposites spectrum, including 1524.63 cm^{-1} (C=C *str.* of cyclic alkanes), 1396.34 cm^{-1} (O-H bend. of phenols) and 881.92 and 667.25 cm^{-1} (C=C bend. of alkenes), support the incorporation of functional groups from the extract onto the synthesized nanocomposites [13,18].

XRD studies: The crystallographic structure of the synthesized Ag-Zn NCs was investigated using X-ray diffraction (XRD) analysis (Fig. 3). The XRD patterns exhibit a combination of diffraction peaks corresponding to both ZnO and Ag phases. Prominent peaks are observed at 2θ values of 31.71º, 34.39º, 36.34º, 47.61º, 56.61º, 62.88º, 66.27º, 67.85º,

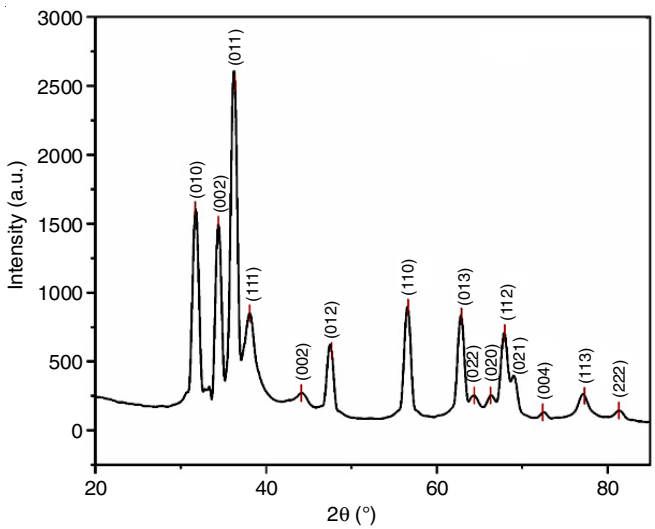

Fig. 3. XRD analysis revealing the planar values of the synthesized Ag-Zn nanocomposite

68.97º and 72.41º. These peaks can be readily indexed to the (010), (002), (011), (012), (110), (013), (020), (112), (021) and (004) planes of a hexagonal wurtzite ZnO structure, in accordance with JCPDS card no. 98-001-1316. Additionally, five distinct peaks were observed at 2θ values of 38.06º, 44.12º, 64.40º, 77.32º and 81.12º, which correspond to the (111), (002), (022), (113) and (222) planes of a face-centered cubic (FCC) silver crystal structure, consistent with JCPDS card no. 98-005-0882. The presence of these peaks confirmed the successful incorporation of silver nanoparticles into the ZnO matrix [18]. Interestingly, the resulted X-ray diffraction (XRD) pattern lacks characteristic peaks associated with potential impurities like Zn, $Zn(OH)_2$ or other silver compounds, suggesting the successful synthesis of pure Ag-Zn NCs without contamination from undesired phases.

The Debye-Scherrer's equation [19] was employed to estimate the average crystallite size of the synthesized Ag-Zn NCs. The equation, $D = 0.9\lambda/\beta \cos\theta$, relates the average crystallite size (D) to the X-ray wavelength (λ), the full width at half maximum (β) of the relevant diffraction peak and the Bragg's diffraction angle (θ). The average crystallite size of the Ag-Zn NCs was calculated to be 6.26 nm.

Morphological studies: The TEM images (Fig. 4) revealed a mixture of nanoscale morphologies, including spherical, hexagonal and rod-shaped nanocomposite. ImageJ software analysis determined an average particle size of 40.37 nm. Furthermore, the majority of the synthesized Ag-Zn NCs exhibited nanoscale dimensions and diverse morphologies, including rods, hexagons and other irregular shapes. Interestingly, a significant portion of the Ag-Zn NCs possessed uniform sizes, with only a small population of larger particles observed. Some agglomeration of particles was evident, a common phenomenon associated with green synthesis methods [20]. This agglomeration can be attributed to the high surface area and inherent stickiness of green-synthesized nanomaterials. Consequently, the ecological factors significantly influence the stability and agglomeration behaviour of nanoparticles. During the formation process, the high affinity between particles leads to the formation of asymmetrical clusters [5,20].

The high-resolution TEM-SAED image further resolves lattice fringes associated with both ZnO and Ag, consistent with the findings from XRD analysis. This visual representation provides additional support for the presence of crystalline phases within the synthesized nanocomposites. Furthermore, analysis of the concentric rings in the SAED pattern allows for calculation of *d*-spacing values. These values matched well with the expected *d*-spacings for the hexagonal wurtzite phase of ZnO and the face-centered cubic (FCC) lattice of silver, as reported by earlier researchers [5,21]. These findings corroborated the XRD data and firmly established the crystalline nature of the individual phases within the Ag-Zn NCs. Therefore, both TEM imaging and SAED analysis provide complementary evidence for the nanocrystallite morphology and poly-crystalline structure of the synthesized Ag-Zn NCs, reaffirming the results obtained from XRD analysis [22].

Photocatalytic degradation of textile dyes: The UV-vis spectroscopy was used to inspect the synthesized Ag-Zn NCs' photocatalytic activity under UV illumination. The four typical dyes were found to have initial maximum absorption wavelengths of 421 nm (RY-86), 409 nm (RY-145), 667 nm (RB-220) and 598 nm (RB-222). Dye degradation was detected by monitoring a decrease in absorption intensity with increasing irradiation time.

As depicted in Fig. 5, the Ag-Zn NCs exhibited remarkable photocatalytic efficiency. They achieved complete degradation (100%) of RB-220 within 160 min of UV irradiation. Similarly, RY-86 and RY-145 also reached complete degradation (100%) within 320 min. Remarkably, RB-222 displayed slightly lower degradation, reaching 87.41% after 320 min of Ag-Zn NCs treatment. These findings demonstrate the promising photocatalytic potential of the synthesized Ag-Zn NCs for treating various dyes, particularly reactive blue and the reactive yellow series. While RB-222 dye degradation was less complete, the achieved percentage highlights the broad activity of the synthesized nanocomposites against different dye molecules. The present findings are further contextualized by comparison with previous studies as detailed in Table-1.

In addition, the photocatalytic activity of the synthesized Ag-Zn NCs was examined using the chemical kinetics analysis. The degradation of each textile dye is illustrated graphically by $\ln(A_t/A_o)$ *vs*. response time in Fig. 6. These plots indicated that the photodegradation process follows pseudo-first-order

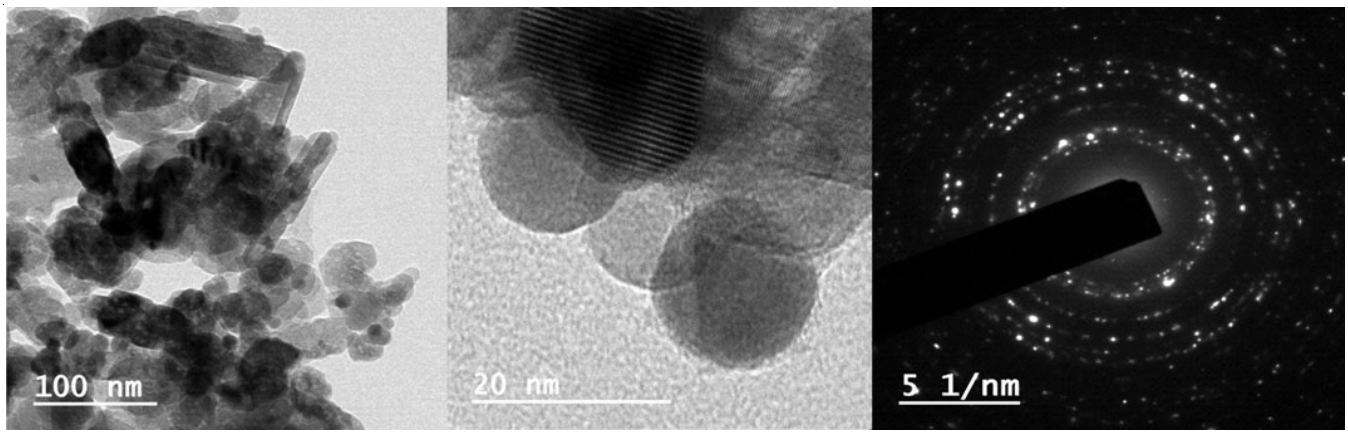

Fig. 4. TEM-SAED images of the synthesized Ag-Zn nanocomposites from *Garcinia indica* leaf extract

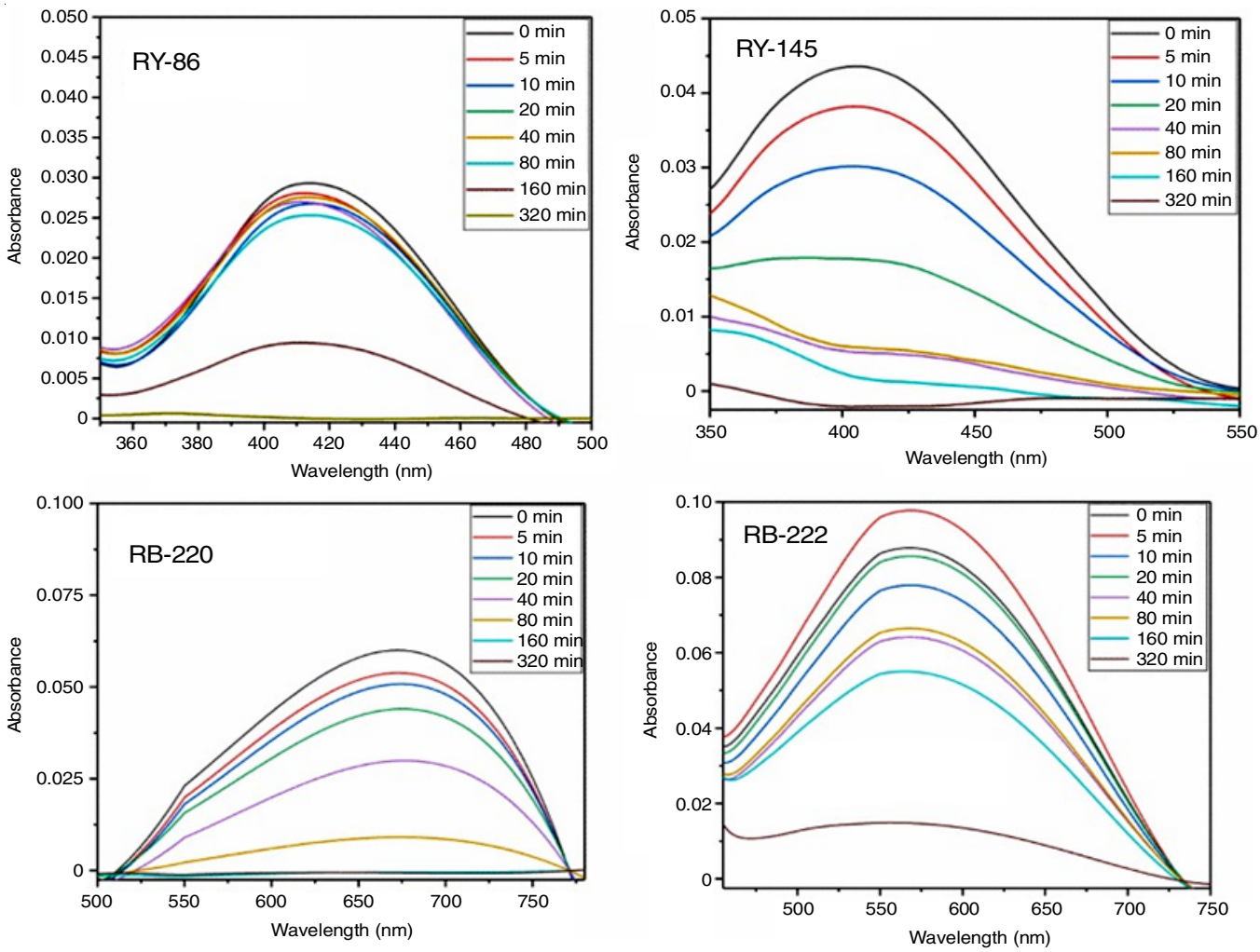

Fig. 5. UV-vis absorption spectrum illustrating the photocatalytic degradation of textile dyes by the synthesized Ag-Zn NCs

TABLE-1
COMPARISON OF NANOCOMPOSITES USED FOR THE PHOTODEGRADATION OF ORGANIC DYE CONTAMINANTS

Nanocomposite	Synthesis method	Dye/contaminant	Light source used	Degradation (%)	Time (min)	Ref.
Ag-ZnO	Green (Goji berry extract)	Methylene blue	Solar light	99.30	90	[5]
		Congo red		98.50	55	
ZnO-Ag	Green *(Carthamus tinctorius L.)*	Methylene blue	UV light	98.00	60	[8]
ZnO-Ag	Green (Gongura leaves)	Methylene blue	UV light	99.21	75	[11]
TiAg	Chemical (Precipitation method)	Methylene blue	Xenon light	97.00	120	[6]
TiAgZnO				99.42	120	
TiZnO				99.85	120	
TiAg	Chemical (Precipitation method)	Rhodamine B	Visible light	40.42	120	[6]
TiAgZnO				87.73	120	
TiZnO				99.29	60	
ZnO-Ag	Green (*T. vulgaris)*	Phenol	Sunlight	97.20	120	[22]
Ag -ZnO	Green (*Trigonella foenum-graceum)*	Malachite green	Visible light	100	120	[17]
Ag-doped ZnO/MgO	Green *(Caccinia macranthera)*	Methylene blue	UV-A	90	120	[23]
Al_2O_3/ZrO_2	Green (Tragacanth gum)	Reactive blue 222 (RB222)	Visible light	91.4	60	[24]
		Reactive yellow 145(RY145)		94.6	60	
GO-TiO_2	Chemical (modified Hummer's method)	Orange ME2RL	UV light	99.6	24	[25]
Ag-ZnO	Green (Potato residues)	Methylene blue	Visible light	96	80	[26]
Ag-ZnO	Green (*Cassia alata)*	Rhodamine 6G	Visible light	-	15	[27]
Ag/ZnO	Green (*Leptadenia pyrotechnica)*	Methyl violet	Solar light	88.93	120	[28]
Ag-Zn	Green (*Garcinia indica)*	Textile reactive dyes	UV light	100	320	Present study

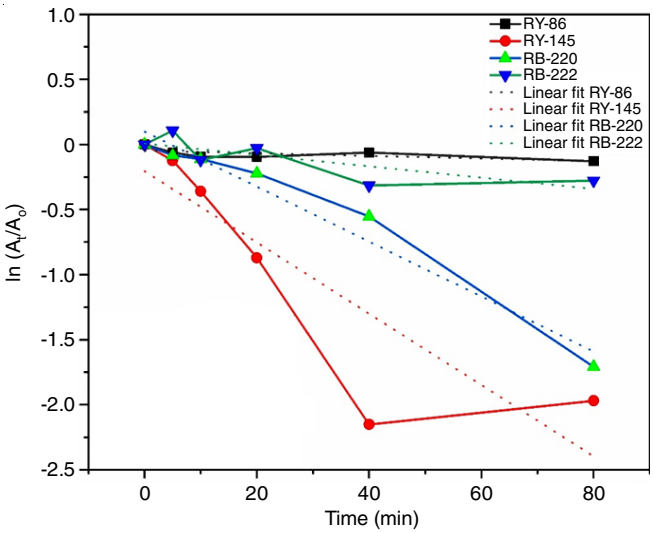

Fig. 6. Plot of $\ln(A_t/A_0)$ *vs.* time showing the photocatalytic degradation of textile dyes by synthesized Ag-Zn nanocomposites following pseudo-first order kinetics

kinetics [6]. The rate constants (k) for each dye were calculated by obtaining the slope of the fitted linear regression lines. The obtained values were 0.000363 min^{-1} for RY-86, 0.000075 min^{-1} for RY-145, 0.000363 min^{-1} for RB-220 and 0.001013 min^{-1} for RB-222. These results suggest that RB-220 exhibits the fastest degradation rate, followed by RY-86 and RY-145. Understanding the kinetic behaviour of the Ag-Zn NCs can help in optimizing their performance and tailoring them for specific wastewater treatment applications.

Conclusion

This study explored the use of *G. indica* leaf aqueous extract for the bioreduction of Ag-Zn nanocomposites. The synthesized nanocomposite were characterized using various spectroscopic and microscopic techniques. The TEM results revealed the mixture of hexagonal, spherical and rod-shaped particles with an average size of 40.37 nm. Importantly, the Ag-Zn nanocomposites demonstrated remarkable photocatalytic activity in degrading reactive textile dyes.

CONFLICT OF INTEREST

The authors declare that there is no conflict of interests regarding the publication of this article.

REFERENCES

1. F.D. Guerra, M.F. Attia, D.C. Whitehead and F. Alexis, *Molecules*, **23**, 1760 (2018); https://doi.org/10.3390/molecules23071760
2. U. Chakraborty, G. Kaur, H.-G. Rubahn, A. Kaushik, G.R. Chaudhary and Y.K. Mishra, *Prog. Mater. Sci.*, **139**, 101169 (2023); https://doi.org/10.1016/j.pmatsci.2023.101169
3. S. Vignesh, P. Eniya, M. Srinivasan, J. Kalyana Sundar, H. Li, S. Jayavel, M. Pandiaraman, M.A. Manthrammel, M. Shkir and B. Palanivel, *J. Environ. Chem. Eng.*, **9**, 105996 (2021); https://doi.org/10.1016/j.jece.2021.105996
4. P. Panchal, R. Sharma, A.S. Reddy, K. Nehra, A. Sharma and S.P. Nehra, *Coord. Chem. Rev.*, **493**, 215283 (2023); https://doi.org/10.1016/j.ccr.2023.215283
5. A.A. Sharwani, K.B. Narayanan, M.E. Khan and S.S. Han, *Sci. Rep.*, **12**, 10017 (2022); https://doi.org/10.1038/s41598-022-14117-w
6. S. Kerli, M. Kavgaci, A.K. Soguksu and B. Avar, *Braz. J. Phys.*, **52**, 22 (2022); https://doi.org/10.1007/s13538-021-01007-1
7. J.T. Kurian, B. Balasubramanian, A. Meyyazhagan, M. Pappuswamy, A.M. Alanazi, K.R.R. Rengasamy, V.A. Arumugam, J.K. Sebastian and J.-T. Chen, *Front. Biosci.-Landmark*, **28**, 169 (2023); https://doi.org/10.31083/j.fbl2808169
8. E.A. Alzahrani, A. Nabi, M.R. Kamli, S.M. Albukhari, S.A. Althabaiti, S.A. Al-Harbi, I. Khan and M.A. Malik, *Water*, **15**, 384 (2023); https://doi.org/10.3390/w15030384
9. J. Sharma, S. Sharma and V. Soni, *Reg. Stud. Mar. Sci.*, **45**, 101802 (2021); https://doi.org/10.1016/j.rsma.2021.101802
10. P.C. Nagajyothi, S.V. Prabhakar Vattikuti, K.C. Devarayapalli, K. Yoo, J. Shim and T.V.M. Sreekanth, *Crit. Rev. Environ. Sci. Technol.*, **50**, 2617 (2020); https://doi.org/10.1080/10643389.2019.1705103
11. P. Jadhav, S. Shinde, S.S. Suryawanshi, S.B. Teli, P.S. Patil, A.A. Ramteke, N.G. Hiremath and R. Prasad, *Eng. Sci.*, (2020); https://doi.org/10.30919/es8d1138
12. S.H. Lim, H.S. Lee, C.H. Lee and C.-I. Choi, *Pharmaceuticals*, **14**, 1338 (2021); https://doi.org/10.3390/ph14121338
13. N.A. Sarip, N.I. Aminudin and W.H. Danial, *Environ. Chem. Lett.*, **20**, 469 (2022); https://doi.org/10.1007/s10311-021-01319-3
14. P. Karthiga, *Biotechnol. Res. Innov.*, **2**, 30 (2018); https://doi.org/10.1016/j.biori.2017.11.001
15. E. Gurgur, S.S. Oluyamo, A.O. Adetuyi, O.I. Omotunde and A.E. Okoronkwo, *SN Appl. Sci.*, **2**, 911 (2020); https://doi.org/10.1007/s42452-020-2269-3
16. R. Rathnasamy, P. Thangasamy, R. Thangamuthu, S. Sampath and V. Alagan, *J. Mater. Sci. Mater. Electron.*, **28**, 10374 (2017); https://doi.org/10.1007/s10854-017-6807-8
17. Z. Noohpisheh, H. Amiri, S. Farhadi and A. Mohammadi-gholami, *Spectrochim. Acta A Mol. Biomol. Spectrosc.*, **240**, 118595 (2020); https://doi.org/10.1016/j.saa.2020.118595
18. D.S. Arumai Selvan, M. Keerthi, S. Murugesan, S. Shobana, B. Lakshmi, V. Veena and A.K. Rahiman, *Mater. Chem. Phys.*, **272**, 124903 (2021); https://doi.org/10.1016/j.matchemphys.2021.124903
19. B. Ajitha, Y.A.K. Reddy and P.S. Reddy, *Spectrochim. Acta A Mol. Biomol. Spectrosc.*, **121**, 164 (2014); https://doi.org/10.1016/j.saa.2013.10.077
20. M.A. Mousa, A. El Nemr, E.A. Gomaa, S.M. Eldafrawy and E.T. Helmy, *Egypt. J. Aquat. Biol. Fish.*, **22**, 149 (2018); https://doi.org/10.21608/ejabf.2018.8343
21. M. Aminuzzaman, L.P. Ying, W.-S. Goh and A. Watanabe, *Bull. Mater. Sci.*, **41**, 50 (2018); https://doi.org/10.1007/s12034-018-1568-4
22. M. Zare, K. Namratha, S. Alghamdi, Y.H.E. Mohammad, A. Hezam, M. Zare, Q.A. Drmosh, K. Byrappa, B.N. Chandrashekar, S. Ramakrishna and X. Zhang, *Sci. Rep.*, **9**, 8303 (2019); https://doi.org/10.1038/s41598-019-44309-w
23. Z. Sabouri, S. Sabouri, S.S.T.H. Moghaddas, A. Mostafapour, S.M. Gheibihayat and M. Darroudi, *Biomass Convers. Biorefinery*, **14**, 2893 (2024); https://doi.org/10.1007/s13399-022-02907-1
24. A. Yaghoubi, A. Ramazani and S. Taghavi-Fardood, *ChemistrySelect*, **5**, 9966 (2020); https://doi.org/10.1002/slct.202002578
25. V. Kumaran, S. P, A. Konga and G. Ponniah, *Pol. J. Environ. Stud.*, **29**, 1683 (2020); https://doi.org/10.15244/pjoes/109027
26. F.A. Alharthi, A.A. Alghamdi, N. Al-Zaqri, H.S. Alanazi, A.A. Alsyahi, A.E. Marghany and N. Ahmad, *Sci. Rep.*, **10**, 20229 (2020); https://doi.org/10.1038/s41598-020-77426-y
27. K. Nagaraj, J. Naman, M. Dixitkumar, P. Thangamuniyandi, S.R. Panda, S. Kamalesu, J. Priyanshi, S. Lokhandwala, N.M. Parekh, T.-W. Chiu, S. Sakthinathan, C. Karuppiah, A. Karthikeyan and I.K. Selvam, *Inorg. Chem. Commun.*, **151**, 110635 (2023); https://doi.org/10.1016/j.inoche.2023.110635
28. M. Afzal, M. Javed, S. Aroob, T. Javed, M.M. Alnoman, W. Alelwani, I. Bibi, M. Sharif, M. Saleem, M. Rizwan, A. Raheel, I. Maseeh, S. Carabineiro and M. Taj, *Nanomaterials*, **13**, 2079 (2023); https://doi.org/10.3390/nano13142079